Scalar Field Perturbations and Quasinormal Modes in AdS_3 and BTZ Spacetimes

Independent Study

Puja Mandal

JULY 2025-Ongoing

1 Klein–Gordon Equation in Flat and Curved Spacetime

1.1 Action and Equation of Motion in Minkowski Spacetime

We consider a real scalar field $\phi(x)$ defined on Minkowski spacetime with metric

$$\eta_{\mu\nu} = \mathrm{diag}(-1, +1, +1, +1).$$

The action for a free scalar field is

$$S = \int d^4x \left[\frac{1}{2} \eta^{\mu\nu} \partial_\mu \phi \, \partial_\nu \phi - \frac{1}{2} m^2 \phi^2 \right]. \tag{1}$$

Varying the action with respect to ϕ and applying the Euler–Lagrange equation,

$$\frac{\partial \mathcal{L}}{\partial \phi} - \partial_\mu \left(\frac{\partial \mathcal{L}}{\partial(\partial_\mu \phi)} \right) = 0,$$

yields the Klein–Gordon equation

$$(\Box + m^2)\phi = 0, \qquad \Box = \eta^{\mu\nu} \partial_\mu \partial_\nu. \tag{2}$$

1.2 Plane–Wave Solutions in Minkowski Spacetime

We consider the plane–wave ansatz

$$\phi(x) = e^{-ik_\mu x^\mu} = e^{-i(\omega t - \mathbf{k}\cdot\mathbf{x})}. \tag{3}$$

Computing derivatives,

$$\partial_\mu \phi = -ik_\mu \phi, \qquad \partial_\mu \partial_\nu \phi = -k_\mu k_\nu \phi.$$

Substituting into the Klein–Gordon equation gives

$$(\eta^{\mu\nu}k_\mu k_\nu - m^2)\phi = 0.$$

Using $\eta^{\mu\nu}k_\mu k_\nu = -\omega^2 + \mathbf{k}^2$, we obtain the dispersion relation

$$\omega^2 = \mathbf{k}^2 + m^2. \tag{4}$$

Thus, plane waves are exact solutions of the Klein–Gordon equation in Minkowski spacetime.

1.3 Scalar Field Lagrangian in Curved Spacetime

Let $\phi(x)$ be a real scalar field on a spacetime manifold with metric $g_{\mu\nu}(x)$.

Generalization to curved spacetime

In curved spacetime, Lorentz invariance is replaced by general covariance. The following replacements are required:

$$\eta_{\mu\nu} \to g_{\mu\nu}(x), \tag{5}$$

$$\eta^{\mu\nu} \to g^{\mu\nu}(x), \tag{6}$$

$$d^4x \to d^4x\,\sqrt{-g}, \tag{7}$$

where

$$g = \det(g_{\mu\nu}).$$

Since ϕ is a scalar,

$$\nabla_\mu \phi = \partial_\mu \phi.$$

Curved-spacetime Lagrangian density

The kinetic term is constructed as

$$g^{\mu\nu}(x)\partial_\mu\phi\,\partial_\nu\phi, \tag{8}$$

and the mass term remains

$$m^2\phi^2. \tag{9}$$

Thus, the Lagrangian density is

$$\mathcal{L} = \frac{1}{2}g^{\mu\nu}(x)\partial_\mu\phi\,\partial_\nu\phi - \frac{1}{2}m^2\phi^2. \tag{10}$$

Action in curved spacetime

The generally covariant action is

$$S = \int d^4x\,\sqrt{-g}\left[\frac{1}{2}g^{\mu\nu}\partial_\mu\phi\,\partial_\nu\phi - \frac{1}{2}m^2\phi^2\right]. \tag{11}$$

In the limit $g_{\mu\nu} \to \eta_{\mu\nu}$, this action reduces to the flat-spacetime scalar field action.

1.4 Derivation of the Curved–Spacetime Klein–Gordon Equation

Varying the action with respect to ϕ,

$$\phi \to \phi + \delta\phi,$$

we obtain

$$\delta S = \int d^4x \, \sqrt{-g} \left[g^{\mu\nu} \partial_\mu \phi \, \partial_\nu (\delta\phi) - m^2 \phi \, \delta\phi \right].$$

Integrating by parts and discarding boundary terms,

$$\delta S = -\int d^4x \left[\partial_\mu (\sqrt{-g}\, g^{\mu\nu} \partial_\nu \phi) + \sqrt{-g}\, m^2 \phi \right] \delta\phi.$$

Requiring $\delta S = 0$ for arbitrary $\delta\phi$ yields

$$\frac{1}{\sqrt{-g}} \partial_\mu \left(\sqrt{-g}\, g^{\mu\nu} \partial_\nu \phi \right) - m^2 \phi = 0. \tag{12}$$

Defining the curved d'Alembertian,

$$\Box_g = \frac{1}{\sqrt{-g}} \partial_\mu \left(\sqrt{-g}\, g^{\mu\nu} \partial_\nu \right),$$

the equation of motion takes the form

$$(\Box_g - m^2)\phi = 0. \tag{13}$$

1.5 Failure of Plane–Wave Solutions in Curved Spacetime

We now attempt the same plane–wave ansatz,

$$\phi(x) = e^{-ik_\mu x^\mu}, \tag{14}$$

where k_μ is constant.

Then

$$\partial_\nu \phi = -ik_\nu \phi.$$

Substituting into the curved d'Alembertian,

$$\Box_g \phi = \frac{1}{\sqrt{-g}} \partial_\mu \left(-i\sqrt{-g}\, g^{\mu\nu} k_\nu \phi \right).$$

Applying the product rule,

$$\Box_g \phi = -\frac{i}{\sqrt{-g}} (\partial_\mu (\sqrt{-g}\, g^{\mu\nu})) k_\nu \phi - g^{\mu\nu}(x) k_\mu k_\nu \phi.$$

Hence,

$$(\Box_g - m^2)\phi = \left[-g^{\mu\nu}(x) k_\mu k_\nu - i \frac{1}{\sqrt{-g}} (\partial_\mu (\sqrt{-g}\, g^{\mu\nu})) k_\nu - m^2 \right] \phi. \tag{15}$$

Since $\partial_\mu (\sqrt{-g}\, g^{\mu\nu}) \neq 0$ in a generic curved spacetime, the equation does not reduce to an algebraic dispersion relation. Therefore, plane–wave solutions of the form $e^{-ik_\mu x^\mu}$ do not solve the Klein–Gordon equation in curved spacetime.

2 Dependence of the Klein–Gordon Equation on Spacetime Geometry

The dynamics of a scalar field ϕ on a given spacetime background $(\mathcal{M}, g_{\mu\nu})$ is governed by the minimally coupled Klein–Gordon equation

$$(\Box_g - m^2)\phi = 0, \tag{16}$$

where $\Box_g$ is the covariant d'Alembertian operator associated with the spacetime metric $g_{\mu\nu}$.

The explicit form of $\Box_g$ depends entirely on the underlying geometry and is given, for a scalar field, by

$$\Box_g \phi = \frac{1}{\sqrt{-g}} \partial_\mu \left(\sqrt{-g}\, g^{\mu\nu} \partial_\nu \phi \right), \tag{17}$$

where $g = \det(g_{\mu\nu})$. Thus, different spacetime geometries lead to different differential operators and consequently to different solution spaces of the Klein–Gordon equation.

2.1 Flat Minkowski Spacetime

In flat spacetime with metric

$$g_{\mu\nu} = \eta_{\mu\nu} = \mathrm{diag}(-1, 1, 1, 1), \tag{18}$$

the determinant is $\sqrt{-g} = 1$ and the inverse metric is constant. The d'Alembertian reduces to

$$\Box = \eta^{\mu\nu} \partial_\mu \partial_\nu = -\partial_t^2 + \nabla^2. \tag{19}$$

The Klein–Gordon equation becomes

$$(-\partial_t^2 + \nabla^2 - m^2)\phi = 0, \tag{20}$$

which admits plane wave solutions

$$\phi(x) = e^{-ik_\mu x^\mu}, \qquad k^2 = -m^2. \tag{21}$$

2.2 General Curved Spacetime

For a general curved spacetime with metric $g_{\mu\nu}(x)$, the Klein–Gordon equation takes the form

$$\frac{1}{\sqrt{-g}} \partial_\mu \left(\sqrt{-g}\, g^{\mu\nu} \partial_\nu \phi \right) - m^2 \phi = 0. \tag{22}$$

In this case, the coefficients of the differential operator are coordinate dependent, and plane wave solutions are no longer eigenfunctions of $\Box_g$.

2.3 Friedmann–Robertson–Walker Spacetime

For a spatially flat FRW spacetime with metric

$$ds^2 = -dt^2 + a(t)^2 d\vec{x}^2, \tag{23}$$

one finds

$$\Box_g \phi = -\partial_t^2 \phi - 3\frac{\dot{a}}{a}\partial_t \phi + \frac{1}{a(t)^2}\nabla^2 \phi. \tag{24}$$

The Klein–Gordon equation explicitly contains time-dependent coefficients induced by the expanding geometry.

2.4 Anti–de Sitter Spacetime

In Anti–de Sitter spacetime, the metric components and the determinant are nontrivial functions of the coordinates, leading to a d'Alembertian operator with variable coefficients. As a result, the Klein–Gordon equation becomes a nontrivial partial differential equation whose solutions differ qualitatively from plane waves.

This dependence of $\Box_g$ on the spacetime geometry motivates the study of scalar field dynamics on highly symmetric curved backgrounds, such as Anti–de Sitter space, where the equation remains analytically tractable despite the presence of curvature.

2.5 Covariant d'Alembertian in Anti–de Sitter Spacetime

We now specialize to Anti–de Sitter spacetime in global coordinates. For AdS_3, the metric is given by

$$ds^2 = L^2\left(-\cosh^2\rho\, dt^2 + d\rho^2 + \sinh^2\rho\, d\phi^2\right), \tag{25}$$

where L denotes the AdS radius.

From the line element, the metric components are

$$g_{\mu\nu} = L^2 \begin{pmatrix} -\cosh^2\rho & 0 & 0 \\ 0 & 1 & 0 \\ 0 & 0 & \sinh^2\rho \end{pmatrix}, \tag{26}$$

with inverse metric

$$g^{\mu\nu} = \frac{1}{L^2} \begin{pmatrix} -\dfrac{1}{\cosh^2\rho} & 0 & 0 \\ 0 & 1 & 0 \\ 0 & 0 & \dfrac{1}{\sinh^2\rho} \end{pmatrix}. \tag{27}$$

The determinant of the metric is

$$g = -L^6 \cosh^2\rho \sinh^2\rho, \tag{28}$$

so that

$$\sqrt{-g} = L^3 \cosh\rho \sinh\rho. \tag{29}$$

The covariant d'Alembertian acting on a scalar field ϕ is defined as

$$\Box_g \phi = \frac{1}{\sqrt{-g}} \partial_\mu \left(\sqrt{-g}\, g^{\mu\nu} \partial_\nu \phi \right). \tag{30}$$

Substituting the AdS_3 metric data, we obtain

$$\Box_g \phi = \frac{1}{L^3 \cosh\rho \sinh\rho} \partial_t \left(-\frac{L \sinh\rho}{\cosh\rho}\, \partial_t \phi \right) + \frac{1}{L^3 \cosh\rho \sinh\rho} \partial_\rho \left(L \cosh\rho \sinh\rho\, \partial_\rho \phi \right) + \frac{1}{L^3 \cosh\rho \sinh\rho} \partial_\phi \left(\frac{L \cosh\rho}{\sinh\rho}\, \partial_\phi \phi \right). \tag{31}$$

Simplifying, the d'Alembertian in global AdS_3 takes the form

$$\boxed{\Box_g \phi = -\frac{1}{L^2 \cosh^2\rho}\, \partial_t^2 \phi + \frac{1}{L^2 \sinh\rho \cosh\rho} \partial_\rho \left(\sinh\rho \cosh\rho\, \partial_\rho \phi \right) + \frac{1}{L^2 \sinh^2\rho}\, \partial_\phi^2 \phi.} \tag{32}$$

3 Scalar Field Dynamics in Global AdS_3

We now study the dynamics of a scalar field propagating on a fixed Anti–de Sitter background. Throughout this section we work in global coordinates on AdS_3.

3.1 Geometry of Global AdS_3

The metric of AdS_3 in global coordinates (t, ρ, ϕ) is given by

$$ds^2 = L^2 \left(-\cosh^2\rho\, dt^2 + d\rho^2 + \sinh^2\rho\, d\phi^2 \right), \tag{33}$$

where L denotes the AdS radius.

The corresponding metric components are

$$g_{\mu\nu} = L^2 \begin{pmatrix} -\cosh^2\rho & 0 & 0 \\ 0 & 1 & 0 \\ 0 & 0 & \sinh^2\rho \end{pmatrix}, \tag{34}$$

with inverse metric

$$g^{\mu\nu} = \frac{1}{L^2} \begin{pmatrix} -\dfrac{1}{\cosh^2\rho} & 0 & 0 \\ 0 & 1 & 0 \\ 0 & 0 & \dfrac{1}{\sinh^2\rho} \end{pmatrix}. \tag{35}$$

The determinant of the metric is

$$g = -L^6 \cosh^2\rho \sinh^2\rho, \tag{36}$$

so that

$$\sqrt{-g} = L^3 \cosh\rho \sinh\rho. \tag{37}$$

3.2 Covariant d'Alembertian in AdS_3

For a scalar field ϕ, the covariant d'Alembertian is defined as

$$\Box_g \phi = \frac{1}{\sqrt{-g}} \partial_\mu \left(\sqrt{-g}\, g^{\mu\nu} \partial_\nu \phi \right). \tag{38}$$

Substituting the AdS_3 metric data, one finds

$$\Box_g \phi = -\frac{1}{L^2 \cosh^2\rho}\, \partial_t^2 \phi + \frac{1}{L^2 \sinh\rho \cosh\rho} \partial_\rho \left(\sinh\rho \cosh\rho\, \partial_\rho \phi \right) + \frac{1}{L^2 \sinh^2\rho}\, \partial_\phi^2 \phi. \tag{39}$$

3.3 Klein–Gordon Equation in AdS_3

The minimally coupled Klein–Gordon equation is

$$(\Box_g - m^2)\phi = 0. \tag{40}$$

Using the explicit form of $\Box_g$, this becomes

$$\begin{aligned} &-\frac{1}{\cosh^2\rho}\, \partial_t^2 \phi + \frac{1}{\sinh\rho \cosh\rho} \partial_\rho \left(\sinh\rho \cosh\rho\, \partial_\rho \phi \right) + \frac{1}{\sinh^2\rho}\, \partial_\phi^2 \phi \\ &\quad - m^2 L^2\, \phi = 0. \end{aligned} \tag{41}$$

3.4 Separation of Variables

The AdS_3 metric is invariant under time translations and rotations in ϕ. We therefore seek separable solutions of the form

$$\phi(t, \rho, \phi) = e^{-i\omega t}\, e^{i\ell\phi}\, R(\rho), \qquad \ell \in \mathbb{Z}. \tag{42}$$

Substituting this ansatz into the Klein–Gordon equation yields a radial ordinary differential equation for $R(\rho)$:

$$\boxed{\frac{1}{\sinh\rho \cosh\rho} \frac{d}{d\rho} \left(\sinh\rho \cosh\rho \frac{dR}{d\rho} \right) - \left(\frac{\omega^2}{\cosh^2\rho} - \frac{\ell^2}{\sinh^2\rho} + m^2 L^2 \right) R(\rho) = 0.} \tag{43}$$

3.5 Asymptotic Analysis of the Radial Equation

We now analyze the behavior of solutions of the radial equation

$$\frac{1}{\sinh\rho\,\cosh\rho}\frac{d}{d\rho}\left(\sinh\rho\,\cosh\rho\,\frac{dR}{d\rho}\right)-\left(\frac{\omega^2}{\cosh^2\rho}-\frac{\ell^2}{\sinh^2\rho}+m^2L^2\right)R(\rho)=0 \tag{44}$$

in the limits $\rho\to 0$ and $\rho\to\infty$.

3.5.1 Behavior Near the Origin $\rho\to 0$

Near the origin, the hyperbolic functions behave as

$$\sinh\rho\sim\rho,\qquad \cosh\rho\sim 1. \tag{45}$$

In this limit, the radial equation reduces to

$$\frac{1}{\rho}\frac{d}{d\rho}\left(\rho\,\frac{dR}{d\rho}\right)-\frac{\ell^2}{\rho^2}R\simeq 0. \tag{46}$$

We seek power-law solutions of the form

$$R(\rho)\sim\rho^{\alpha}. \tag{47}$$

Substituting into the equation yields

$$\alpha(\alpha-1)+\alpha-\ell^2=0, \tag{48}$$

which gives

$$\alpha^2=\ell^2. \tag{49}$$

Thus, the two independent solutions behave as

$$R(\rho)\sim\rho^{\pm|\ell|}. \tag{50}$$

Regularity at the origin requires

$$R(\rho)\sim\rho^{|\ell|}. \tag{51}$$

3.5.2 Behavior Near the Boundary $\rho\to\infty$

For large ρ, the hyperbolic functions asymptote to

$$\sinh\rho\sim\cosh\rho\sim\tfrac{1}{2}e^{\rho}. \tag{52}$$

In this limit, the radial equation simplifies to

$$\frac{d^2R}{d\rho^2}+2\,\frac{dR}{d\rho}-m^2L^2\,R\simeq 0. \tag{53}$$

We consider exponential solutions of the form

$$R(\rho) \sim e^{-\Delta\rho}. \tag{54}$$

Substituting into the equation gives the characteristic equation

$$\Delta(\Delta - 2) = m^2 L^2. \tag{55}$$

Solving for Δ, we obtain

$$\Delta_\pm = 1 \pm \sqrt{1 + m^2 L^2}. \tag{56}$$

Therefore, near the AdS boundary, the scalar field behaves as

$$R(\rho) \sim A\, e^{-\Delta_- \rho} + B\, e^{-\Delta_+ \rho}. \tag{57}$$

4 Radial Equation

The dynamics of the scalar field in global AdS_3 is thus encoded in the radial ordinary differential equation

$$\frac{1}{\sinh\rho\,\cosh\rho}\frac{d}{d\rho}\left(\sinh\rho\,\cosh\rho\,\frac{dR}{d\rho}\right) - \left(\frac{\omega^2}{\cosh^2\rho} - \frac{\ell^2}{\sinh^2\rho} + m^2L^2\right)R(\rho) = 0, \tag{58}$$

which will be the central object of analysis in the following sections.

4.1 Boundary Conditions and Physical Admissibility

The asymptotic analysis of the radial equation reveals that the scalar field solutions in global AdS_3 are strongly constrained by the geometry of the spacetime. In particular, physical admissibility requires regularity of the scalar field in the interior and normalizability at the asymptotic AdS boundary.

4.1.1 Regularity at the Origin

Near the origin $\rho \to 0$, the radial equation admits solutions of the form

$$R(\rho) \sim \rho^{\pm|\ell|}. \tag{59}$$

Requiring the scalar field to remain finite at the origin excludes the divergent solution. Thus, regularity uniquely selects

$$R(\rho) \sim \rho^{|\ell|}. \tag{60}$$

4.1.2 Normalizability at the AdS Boundary

Near the AdS boundary $\rho \to \infty$, the scalar field behaves as

$$R(\rho) \sim A\, e^{-\Delta_- \rho} + B\, e^{-\Delta_+ \rho}, \qquad \Delta_\pm = 1 \pm \sqrt{1 + m^2 L^2}. \tag{61}$$

Physical solutions must be normalizable with respect to the inner product induced by the AdS_3 metric. Stability further requires that the scalar mass satisfy the Breitenlohner–Freedman bound

$$m^2 L^2 \geq -1. \tag{62}$$

For generic masses, only the faster decaying mode $e^{-\Delta_+ \rho}$ is normalizable, leading to the boundary condition $A = 0$. In the mass range $-1 < m^2 L^2 < 0$, both fall-off modes are normalizable, allowing for alternative quantization schemes. In this work, we adopt the standard quantization.

4.1.3 Physical Interpretation

The combined requirements of regularity at the origin and normalizability at the AdS boundary restrict the scalar field to a discrete set of smooth, finite-energy configurations. The timelike nature of the AdS boundary leads to reflective boundary conditions, preventing energy loss and implying a discrete normal mode spectrum.

This analysis motivates the explicit determination of the normal mode frequencies in the following section.

5 Normal Mode Spectrum in Global AdS_3

We now determine the allowed frequency spectrum of the scalar field by solving the radial equation subject to the boundary conditions derived in the previous section. Regularity at the origin and normalizability at the AdS boundary together lead to a discrete set of normal modes.

5.1 Reduction of the Radial Equation

It is convenient to introduce the dimensionless variable

$$z = \tanh^2 \rho, \qquad 0 \leq z < 1, \tag{63}$$

where $z = 0$ corresponds to the origin and $z \to 1$ to the AdS boundary. Using

$$\sinh^2 \rho = \frac{z}{1-z}, \qquad \cosh^2 \rho = \frac{1}{1-z}, \tag{64}$$

the radial equation can be rewritten in terms of the variable z.

Motivated by the asymptotic analysis, we factor out the known behavior at the singular points and write the radial function as

$$R(\rho) = z^{\frac{|\ell|}{2}}(1-z)^{\frac{\Delta_+}{2}} F(z), \qquad \Delta_+ = 1 + \sqrt{1+m^2L^2}. \tag{65}$$

Substituting this ansatz into the radial equation, one finds that the function $F(z)$ satisfies the Gauss hypergeometric equation

$$z(1-z)\frac{d^2F}{dz^2} + [c-(a+b+1)z]\,\frac{dF}{dz} - ab\,F = 0, \tag{66}$$

with parameters

$$a = \frac{1}{2}\left(\Delta_+ + |\ell| - \omega\right), \qquad b = \frac{1}{2}\left(\Delta_+ + |\ell| + \omega\right), \qquad c = 1 + |\ell|. \tag{67}$$

The general solution is therefore given by the hypergeometric function

$$F(z) = {}_2F_1(a,b;c;z). \tag{68}$$

5.2 Quantization Condition

The remaining boundary condition is imposed at the AdS boundary, corresponding to the limit $z \to 1$. In general, the hypergeometric function ${}_2F_1(a,b;c;z)$ diverges as $z \to 1$. Normalizability of the scalar field therefore requires that the hypergeometric series truncate to a polynomial.

This truncation occurs if and only if one of the parameters a or b is a non-positive integer. Choosing

$$a = -n, \qquad n = 0, 1, 2, \ldots \tag{69}$$

ensures that the solution reduces to a polynomial of degree n and remains finite at the boundary.

5.3 Discrete Normal Mode Spectrum

Using the definition of a, the quantization condition implies

$$\frac{1}{2}\left(\Delta_+ + |\ell| - \omega\right) = -n. \tag{70}$$

Solving for ω, we obtain the discrete normal mode spectrum

$$\boxed{\omega_{n,\ell} = \Delta_+ + |\ell| + 2n, \qquad n = 0, 1, 2, \ldots} \tag{71}$$

The spectrum is real and equally spaced, reflecting the absence of dissipation in global AdS_3. The corresponding eigenfunctions are regular at the origin and decay exponentially at the AdS boundary, forming a complete set of normal modes for the scalar field.

6 Numerical Verification of the Normal Mode Spectrum

To complement the analytical derivation of the normal mode spectrum, we numerically solved the radial Klein–Gordon equation in global AdS_3. The radial equation was treated as an eigenvalue problem for the frequency ω, subject to the boundary conditions derived earlier.

6.1 Numerical Method

The radial equation was rewritten as a system of first-order ordinary differential equations and integrated using a shooting method. Near the origin, regularity was imposed by initializing the solution as

$$R(\rho) \sim \rho^{|\ell|}, \qquad \frac{dR}{d\rho} \sim |\ell|\, \rho^{|\ell|-1}, \tag{72}$$

at a small radial cutoff $\rho = \varepsilon \ll 1$.

The equation was then integrated outward to a large radial cutoff $\rho = \rho_{\max}$, chosen such that the asymptotic behavior of the solution was well approximated by its boundary form. Normalizable solutions were identified by requiring exponential decay of the radial function at large ρ.

7 Numerical Verification

To verify the analytical normal mode spectrum derived above, the radial Klein–Gordon equation in global AdS_3 was solved numerically using a shooting method.
...

For the case $m^2 = 0$ and $\ell = 0$, the numerical shooting method yields the lowest normal mode frequencies $\omega \approx 2.00$, 4.00, 6.00, and 8.00 for $n = 0, 1, 2,$ and 3, respectively. These values are in exact agreement with the analytical prediction

$$\omega_{n,\ell} = \Delta_+ + |\ell| + 2n, \tag{73}$$

thereby confirming the quantization of the spectrum.

Representative numerical eigenfunctions are shown in Fig. 1. The solutions exhibit smooth behavior at the origin, an increasing number of radial nodes with increasing n, and exponential decay near the AdS boundary.

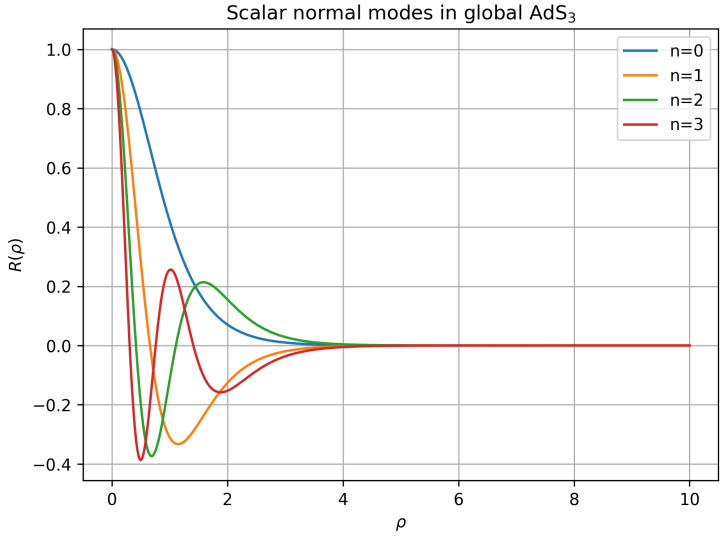

Figure 1: Numerically computed radial eigenfunctions $R(\rho)$ for the lowest scalar normal modes in global AdS_3 with $m^2 = 0$ and $\ell = 0$. The number of nodes increases with the radial quantum number n, and all modes are regular at the origin and decay exponentially toward the AdS boundary.

8 Motivation

Black holes provide a unique arena for testing fundamental theories of gravity and quantum mechanics, particularly in strong-field regimes where classical and quantum effects interplay nontrivially. Understanding their dynamical behavior is therefore of central importance in gravitational physics.

Since black holes are not isolated systems, their interaction with external disturbances such as infalling matter or gravitational radiation naturally leads to the study of black hole perturbations. The response of a black hole to such perturbations is governed by *quasinormal modes* (QNMs), which are characteristic damped oscillations dominating the late-time evolution of the system. These modes are universal in nature, depending only on the intrinsic parameters of the black hole, such as mass, charge, and angular momentum, and not on the details of the initial perturbation.

The spectrum of quasinormal frequencies encodes crucial information about the stability of the underlying spacetime and plays a vital role in gravitational wave physics, particularly in the analysis of black hole ringdown signals.

In this project, special attention is given to the *BTZ black hole*, a $(2+1)$-dimensional solution of Einstein gravity with a negative cosmological constant. Despite its lower dimensionality, the BTZ black hole shares many essential thermodynamical and geometrical features with higher-dimensional black holes. Owing to its relative mathematical simplicity, it serves as a valuable toy

model for exploring black hole dynamics, especially within the framework of the AdS/CFT correspondence.

Motivated by these considerations, this work aims to investigate black hole perturbations and quasinormal modes in the BTZ background as a means to gain deeper insight into spacetime stability and holographic aspects of gravity.

9 Objectives and Scope of the Independent Study

The primary aim of this independent study is to explore the behavior of scalar field perturbations in the background of the BTZ black hole and to understand the emergence of quasinormal modes from such perturbations. Rather than focusing solely on final numerical results, the emphasis is placed on developing analytical insight into the underlying structure of the wave equations and their solutions.

Specifically, this study investigates the dynamics of a (massless) scalar field propagating in the BTZ spacetime by formulating and analyzing the corresponding Klein–Gordon equation. The objective is to derive the characteristic quasinormal mode frequencies and to examine their qualitative and quantitative features, with particular attention to their dependence on the black hole parameters.

From a methodological perspective, the work adopts an analytical approach. The scalar wave equation is studied by relating it to known differential equations appearing in mathematical physics, such as the hypergeometric or Heun equations, allowing the use of established properties of special functions. In parallel, series solution techniques, notably the Frobenius method, are employed to construct solutions near regular singular points and to extract the quasinormal mode conditions through appropriate boundary requirements.

Overall, this independent study aims to provide a self-contained analytical investigation of quasinormal modes in the BTZ black hole background, serving both as a learning exercise in black hole perturbation theory and as a stepping stone toward more advanced studies in AdS/CFT and gravitational wave physics.

10 BTZ Black Hole Background

The Bañados–Teitelboim–Zanelli (BTZ) black hole is a solution of Einstein gravity in (2+1) dimensions with a negative cosmological constant. Although lower-dimensional, it exhibits many of the essential features of higher-dimensional black holes, including horizons, thermodynamics, and well-defined causal structure. Owing to its asymptotically AdS_3 nature, the BTZ spacetime also plays a central role in studies related to the AdS/CFT correspondence.

In its most general form, the BTZ black hole is characterized by a mass M and angular momentum J. In this work, attention is restricted to the non-rotating case ($J = 0$), which provides a technically simpler setting while retain-

ing the key physical aspects relevant for perturbation analysis. The resulting geometry possesses a single event horizon located at $r = r_+$ and serves as the background spacetime for the present investigation.

The global structure of the non-rotating BTZ black hole can be made manifest through suitable coordinate transformations, such as the introduction of tortoise and Kruskal-like coordinates. These constructions allow one to extend the metric across the horizon and to analyze the causal structure using conformal (Penrose) diagrams. The spacetime features a timelike boundary at infinity and a curvature singularity at the origin.

11 Scalar Field Perturbations

To probe the dynamical response of the BTZ black hole, this study considers the propagation of a massless scalar field on the fixed background geometry. The dynamics of the scalar field Φ is governed by the Klein–Gordon equation in curved spacetime,

$$\Box\Phi = \frac{1}{\sqrt{-g}}\partial_\mu\left(\sqrt{-g}\, g^{\mu\nu}\partial_\nu\Phi\right) = 0.$$

Exploiting the symmetries of the background, the scalar field is decomposed into temporal, angular, and radial parts through an appropriate separation of variables. This reduces the problem to an ordinary differential equation for the radial mode function. For analytical convenience, a dimensionless radial coordinate is introduced, mapping the event horizon and the asymptotic boundary to finite values.

The resulting radial equation forms the starting point for the analysis of quasinormal modes, which are obtained by imposing physically motivated boundary conditions: ingoing behavior at the horizon and appropriate fall-off at the asymptotic AdS boundary. These conditions lead to a discrete spectrum of complex frequencies characterizing the decay of scalar perturbations in the BTZ background.

12 Radial Equation for Scalar Perturbations

We consider a massless scalar field Φ propagating on the fixed background of a non-rotating BTZ black hole. The field dynamics is governed by the Klein–Gordon equation

$$\Box\Phi = \frac{1}{\sqrt{-g}}\partial_\mu\left(\sqrt{-g}\, g^{\mu\nu}\partial_\nu\Phi\right) = 0. \tag{74}$$

Exploiting the time-translation and rotational symmetries of the spacetime, we adopt the separation ansatz

$$\Phi(t, r, \chi) = e^{-i\omega t + ip\chi}\,\Psi(r), \tag{75}$$

where ω denotes the frequency and p the angular momentum quantum number.

Introducing the dimensionless radial coordinate

$$y = \frac{r_+^2}{r^2}, \tag{76}$$

the event horizon and asymptotic boundary are mapped to $y = 1$ and $y = 0$, respectively. In terms of this coordinate, the radial equation takes the form

$$y(1-y)\frac{d^2\Psi}{dy^2} - y\frac{d\Psi}{dy} + \left(\frac{\hat{\omega}^2}{1-y} - \hat{p}^2\right)\Psi = 0, \tag{77}$$

where the dimensionless parameters are defined as

$$\hat{\omega} = \frac{\omega}{2r_+}, \qquad \hat{p} = \frac{p}{2r_+}. \tag{78}$$

Equation (77) possesses regular singular points at $y = 0$ and $y = 1$, corresponding to the AdS boundary and the black hole horizon, respectively.

13 Near-Horizon Analysis

Upon separating variables in the Klein–Gordon equation for a massless scalar field propagating in the non-rotating BTZ background, the dynamics reduces to a second-order differential equation governing the radial mode. By introducing a suitable dimensionless radial coordinate, the event horizon and the asymptotic boundary are mapped to finite locations, which simplifies the analytical treatment.

To analyze the behavior of scalar perturbations near the event horizon, we examine the radial equation in the vicinity of $y = 1$. Writing the equation in standard Frobenius form,

$$\frac{d^2\Psi}{dy^2} + P(y)\frac{d\Psi}{dy} + Q(y)\Psi = 0, \tag{79}$$

one finds

$$P(y) = \frac{1}{y-1}, \qquad Q(y) = \frac{\hat{\omega}^2 + \hat{p}^2 y(y-1)}{y^2(y-1)^2}. \tag{80}$$

Since $(y-1)P(y)$ and $(y-1)^2Q(y)$ are analytic at $y = 1$, the horizon is a regular singular point. We therefore seek a Frobenius solution of the form

$$\Psi(y) = (y-1)^\sigma \sum_{n=0}^{\infty} a_n (y-1)^n, \qquad a_0 \neq 0. \tag{81}$$

Substituting this ansatz into the radial equation and retaining the leading-order terms yields the indicial equation

$$\sigma(\sigma-1) + P_0\sigma + Q_0 = 0, \tag{82}$$

where

$$P_0 = \lim_{y\to 1}(y-1)P(y) = 1, \qquad Q_0 = \lim_{y\to 1}(y-1)^2 Q(y) = \hat{\omega}^2. \tag{83}$$

The indicial equation therefore reduces to

$$\sigma^2 + \hat{\omega}^2 = 0, \tag{84}$$

with solutions

$$\sigma_\pm = \pm i\hat{\omega}. \tag{85}$$

The corresponding near-horizon behavior of the scalar field is thus

$$\Psi_\pm(y) \sim (y-1)^{\pm i\hat{\omega}}. \tag{86}$$

The resulting radial equation exhibits singular behavior at specific points corresponding to the horizon and the boundary of the spacetime. In particular, the event horizon appears as a regular singular point of the differential equation, making it amenable to a local series analysis. This structure allows the equation to be related, after appropriate redefinitions, to well-studied classes of differential equations such as the hypergeometric type.

To analyze the behavior of solutions near the horizon, a Frobenius expansion is employed. Assuming a power-law form for the radial function in the vicinity of the horizon leads to an indicial equation that determines the possible leading behaviors of the solution. The corresponding exponents are found to be purely imaginary, reflecting oscillatory behavior near the horizon.

These two independent solutions can be interpreted as ingoing and outgoing modes when translated back to the original spacetime coordinates. For the purpose of defining quasinormal modes, physical considerations dictate the selection of the ingoing solution at the horizon. This boundary condition, together with appropriate asymptotic behavior at infinity, leads to a discrete spectrum of complex frequencies characterizing the decay of scalar perturbations in the BTZ black hole background.

14 Horizon Boundary Condition

Restoring the time dependence $e^{-i\omega t}$, the two independent solutions near the horizon behave as

$$\Phi_\pm \sim e^{-i\omega t}(y-1)^{\pm i\hat{\omega}} = \exp[-i\omega t \pm i\hat{\omega}\ln(y-1)]\,. \tag{87}$$

These solutions correspond to outgoing and ingoing waves at the horizon, respectively. Physical considerations require the exclusion of outgoing modes, as no classical information can escape from the black hole interior. Consequently, the ingoing solution is selected as the physically admissible boundary condition at the horizon.

15 Quantization of Quasinormal Modes

Having determined the admissible behaviors of the scalar field near the event horizon and at the asymptotic AdS boundary, we now derive the quantization condition for quasinormal mode frequencies by constructing a global solution of the radial equation.

We begin with the radial equation obtained after separation of variables,

$$y(1-y)\frac{d^2\Psi}{dy^2} - y\frac{d\Psi}{dy} + \left(\frac{\hat{\omega}^2}{1-y} - \hat{p}^2\right)\Psi = 0, \tag{88}$$

where

$$\hat{\omega} = \frac{\omega}{2r_+}, \qquad \hat{p} = \frac{p}{2r_+}. \tag{89}$$

Equation (88) possesses regular singular points at $y = 0$ and $y = 1$, corresponding to the asymptotic AdS boundary and the event horizon, respectively.

Step 1: Factorization of Singular Behavior

From the Frobenius analysis at the horizon, the scalar field behaves as

$$\Psi(y) \sim (1-y)^{\pm i\hat{\omega}} \quad \text{as } y \to 1. \tag{90}$$

To impose the physically relevant ingoing boundary condition at the horizon, we factor out this behavior and write

$$\Psi(y) = y^{\alpha}(1-y)^{i\hat{\omega}}F(y), \tag{91}$$

where α is a constant to be determined and $F(y)$ is assumed to be regular in the interval $0 < y < 1$.

Step 2: Reduction to Hypergeometric Equation

Substituting the ansatz (91) into the radial equation and simplifying, one finds that the function $F(y)$ satisfies the Gauss hypergeometric equation

$$y(1-y)\frac{d^2F}{dy^2} + \big[c - (a+b+1)y\big]\frac{dF}{dy} - ab\,F = 0, \tag{92}$$

with parameters

$$a = 1 + \alpha + i(\hat{\omega} - \hat{p}), \qquad b = \alpha + i(\hat{\omega} + \hat{p}), \qquad c = 1 + 2\alpha. \tag{93}$$

The general solution regular at the horizon is therefore

$$\Psi(y) = y^{\alpha}(1-y)^{i\hat{\omega}}\,{}_2F_1(a, b; c; y). \tag{94}$$

Step 3: Asymptotic Behavior at the AdS Boundary

To determine the allowed values of α, we examine the behavior of the solution near the AdS boundary $y \to 0$. In this limit,

$$ {}_2F_1(a, b; c; y) \to 1, \tag{95}$$

and the radial function behaves as

$$ \Psi(y) \sim y^{\alpha}. \tag{96}$$

For a massless scalar field in AdS_3, normalizability and finite energy considerations restrict the solution to vanish at the boundary. This requirement fixes

$$ \alpha = 1. \tag{97}$$

Step 4: Polynomial Condition and Frequency Quantization

The hypergeometric function ${}_2F_1(a, b; c; y)$ is generically divergent as $y \to 1$ unless the series truncates to a finite polynomial. Such truncation occurs if either of the parameters a or b is a non-positive integer:

$$ a = -n \quad \text{or} \quad b = -n, \qquad n = 0, 1, 2, \ldots \tag{98}$$

Imposing this condition yields a discrete set of allowed frequencies. Explicitly, one finds

$$ \omega_n^{\pm} = \pm p + i(n+1)r_+, \qquad n = 0, 1, 2, \ldots \tag{99}$$

Equation (99) constitutes the quasinormal mode spectrum for a massless scalar field propagating in the background of a non-rotating BTZ black hole.

16 Quasinormal Mode Spectrum

The quantization condition derived in the previous section leads to a discrete set of complex frequencies characterizing scalar perturbations of the non-rotating BTZ black hole. These frequencies constitute the *quasinormal mode spectrum* of the system.

For a massless scalar field, the quasinormal frequencies are given by

$$ \omega_n^{\pm} = \pm p + i(n+1)r_+, \qquad n = 0, 1, 2, \ldots \tag{100}$$

where p denotes the angular momentum quantum number and n labels the overtone number.

Structure of the Spectrum

The spectrum naturally separates into two branches, corresponding to the $\pm$ signs in Eq. (100). These branches describe modes propagating in opposite angular directions along the boundary of the spacetime and are often referred to as right-moving and left-moving modes, respectively.

Each mode in the spectrum is characterized by a complex frequency

$$\omega = \Re(\omega) + i\,\Im(\omega), \tag{101}$$

where the real part

$$\Re(\omega_n^{\pm}) = \pm p \tag{102}$$

determines the oscillatory behavior of the perturbation, while the imaginary part

$$\Im(\omega_n) = (n+1)r_+ \tag{103}$$

governs the exponential decay rate.

Overtones and Mode Spacing

The integer n labels the overtone number, with the fundamental mode corresponding to $n = 0$. Higher overtones decay more rapidly, as the imaginary part of the frequency increases linearly with n. As a result, the late-time behavior of scalar perturbations is dominated by the lowest-lying mode in the spectrum.

The equally spaced structure of the imaginary parts,

$$\Im(\omega_{n+1}) - \Im(\omega_n) = r_+, \tag{104}$$

is a distinctive feature of the BTZ black hole and reflects the high degree of symmetry of the underlying AdS_3 geometry.

Dimensionless Form of the Spectrum

It is often convenient to express the spectrum in terms of dimensionless quantities by rescaling the frequency with the horizon radius. Defining

$$\hat{\omega} = \frac{\omega}{2r_+}, \qquad \hat{p} = \frac{p}{2r_+}, \tag{105}$$

the spectrum takes the compact form

$$\hat{\omega}_n^{\pm} = \pm\hat{p} + i\,\frac{n+1}{2}. \tag{106}$$

This form highlights the universal spacing of the quasinormal modes and is particularly useful for comparison with analytical and numerical results in other asymptotically AdS spacetimes.

17 Stability and Late-Time Decay

The quasinormal mode spectrum derived in the previous section provides direct insight into the dynamical stability of the BTZ black hole and the late-time behavior of scalar perturbations. Since quasinormal modes govern the response of the spacetime to small disturbances, their frequency structure plays a central role in determining whether perturbations grow or decay with time.

17.1 Stability of the BTZ Black Hole

For scalar perturbations, stability is determined by the sign of the imaginary part of the quasinormal frequencies. Writing the frequency as

$$\omega = \Re(\omega) + i\,\Im(\omega), \tag{107}$$

the time dependence of the perturbation takes the form

$$\Phi(t,\ldots) \sim e^{-i\omega t} = e^{-i\Re(\omega)t}\, e^{-\Im(\omega)t}. \tag{108}$$

A positive imaginary part, $\Im(\omega) > 0$, ensures exponential decay of the perturbation in time, whereas a negative imaginary part would signal an instability.

For the non-rotating BTZ black hole, the quasinormal mode spectrum for a massless scalar field is given by

$$\omega_n^{\pm} = \pm p + i(n+1)r_+, \qquad n = 0, 1, 2, \ldots \tag{109}$$

which implies

$$\Im(\omega_n) = (n+1)r_+ > 0 \quad \text{for all } n. \tag{110}$$

Since the imaginary part is strictly positive for every overtone number, all scalar perturbations decay exponentially in time. This establishes the linear stability of the BTZ black hole under massless scalar field perturbations.

17.2 Role of Overtone Number

The overtone number n labels different quasinormal modes within the spectrum. As n increases, the imaginary part of the frequency grows linearly, leading to faster decay rates for higher overtones. Explicitly,

$$\Im(\omega_{n+1}) - \Im(\omega_n) = r_+, \tag{111}$$

indicating equally spaced decay rates.

As a consequence, higher-overtone modes are rapidly suppressed, and the late-time evolution of the perturbation is dominated by the lowest-lying mode with $n = 0$. This fundamental mode controls the slowest decay rate and sets the characteristic relaxation timescale of the system.

17.3 Late-Time Decay of Scalar Perturbations

At sufficiently late times, the scalar field can be approximated by the contribution of the dominant quasinormal mode,

$$\Phi(t,\ldots) \sim e^{-i\omega_0 t} = e^{-i\Re(\omega_0)t}\, e^{-(r_+)t}, \tag{112}$$

where ω_0 denotes the fundamental frequency.

The late-time behavior is therefore purely exponential, in contrast to the power-law tails commonly observed in asymptotically flat spacetimes. This difference arises from the confining nature of the AdS boundary, which prevents perturbations from dispersing to infinity and leads to a discrete quasinormal spectrum.

The absence of power-law tails and the presence of exponential decay are distinctive features of perturbations in asymptotically AdS black hole backgrounds and reflect the strong influence of the spacetime boundary conditions on the dynamics.

17.4 Summary of Stability Properties

The analysis of the quasinormal mode spectrum demonstrates that the BTZ black hole is dynamically stable against massless scalar perturbations. All modes decay exponentially, with higher overtones decaying more rapidly than the fundamental mode. The late-time evolution is governed entirely by the lowest quasinormal frequency, providing a clear and physically transparent description of relaxation processes in the BTZ background.

18 Future Direction

The immediate future direction of this project is the extension of the present analysis to scalar perturbations in the *rotating BTZ black hole* background. While the non-rotating case provides a clean and analytically tractable setting, the inclusion of angular momentum introduces qualitatively new physical features, such as richer mode structure and the possibility of superradiant behavior.

From a technical perspective, rotation modifies the radial equation and changes the structure of the boundary conditions, requiring a careful reanalysis of the quasinormal mode problem. Investigating how the presence of angular momentum alters the quasinormal mode spectrum and decay rates will allow a direct comparison with the non-rotating case studied in this work.

This extension represents a natural continuation of the current project, using the same analytical framework developed here while exploring a more general and physically rich class of black hole spacetimes.

References

[1] S. M. Carroll, *Spacetime and Geometry: An Introduction to General Relativity*, Addison-Wesley (2004).

[2] A. Sen, *Quantum Field Theory and String Theory*, Cambridge University Press (2016).

[3] S. Mukhi, *String Theory: A Perspective Over the Last 25 Years*, World Scientific (2011).

[4] P. Banerjee, *Lecture Notes on Quantum Field Theory*, ICTS–TIFR, Bangalore. (lecture notes).

[5] M. Bañados, C. Teitelboim and J. Zanelli, "The Black Hole in Three-Dimensional Spacetime," Phys. Rev. Lett. **69**, 1849 (1992).

[6] M. Bañados, M. Henneaux, C. Teitelboim and J. Zanelli, "Geometry of the (2+1)-Dimensional Black Hole," Phys. Rev. D **48**, 1506 (1993).

[7] D. Birmingham, "Choptuik Scaling and Quasinormal Modes in the AdS_3 Black Hole," Phys. Rev. D **64**, 064024 (2001).

[8] V. Cardoso and J. P. S. Lemos, "Quasinormal Modes of the BTZ Black Hole," Phys. Rev. D **63**, 124015 (2001).

[9] G. T. Horowitz and V. E. Hubeny, "Quasinormal Modes of AdS Black Holes and the Approach to Thermal Equilibrium," Phys. Rev. D **62**, 024027 (2000).

[10] P. Breitenlohner and D. Z. Freedman, "Stability in Gauged Extended Supergravity," Annals Phys. **144**, 249 (1982).

[11] R. M. Wald, *General Relativity*, University of Chicago Press (1984).

[12] N. D. Birrell and P. C. W. Davies, *Quantum Fields in Curved Space*, Cambridge University Press (1982).